Chapter 12
Aeroelastic Interactions Between Plates and Three-Dimensional Inviscid Potential Flows

Konstantin V. Avramov, Darkhan S. Myrzaliyev, and Kazira K. Seitkazenova

Abstract The method for analysis of dynamic interactions between plates and three-dimensional, potential, inviscid gas is suggested. The system of the singular integral equations with respect to aerodynamic derivatives of the pressure drop is obtained. The numerical method for the singular integral equations solutions is suggested. Loss of the plate dynamic stability is analyzed numerically.

Keywords Singular integral equation · Inviscid gas · Dynamic instability · Aerodynamic derivative

12.1 Introduction

The singular integral equations with respect to a circulation density are used basically to analyze aeroelasticity of plates in three-dimensional potential flow. In this case, the vorticity shed from the trailing edge of the plate and wake formation are considered. This leads to significant computational burden. The calculations of the plate transient responses reduce to the analysis of the characteristic exponents, which is transformed to high dimension eigenvalue problem (Tang et al. 1999a, b).

K. V. Avramov (✉)
National Academy of Science of Ukraine, Podgorny Institute for Mechanical Engineering, Kharkiv, Ukraine
e-mail: kvavramov@gmail.com

National Technical University "Kharkiv Polytechnic Institute", Kharkiv, Ukraine

Department of Technical Systems, Kharkiv National University of Radio Electronics, Kharkiv, Ukraine

D. S. Myrzaliyev · K. K. Seitkazenova
Department of Mechanics and Engineering, M. Auezov South Kazakhstan State University, Shimkent, Republic of Kazakhstan
e-mail: darkhan-m7@mail.ru

K. K. Seitkazenova
e-mail: kseitkazi@mail.ru

H. Altenbach et al. (eds.), *Nonlinear Mechanics of Complex Structures*, Advanced Structured Materials 157, https://doi.org/10.1007/978-3-030-75890-5_12

In this paper, the singular integral equations with respect to the pressure drop are suggested. The pressure drop outside the plate is equal to zero. Therefore, the wake is not considered. The mechanical steady-state vibrations can be analyzed using single harmonic approximation in time of plate pressure drop. The characteristic exponents are calculated to analyze dynamic stability of the plate. Assuming, that the gas is three-dimensional, potential, inviscid and incompressible, the system of the singular integral equations with respect to the pressure drop is derived. The numerical method for the solutions of the obtained singular integral equations system is suggested.

Now the results of others researchers in this field are considered. The singular integral equation with respect to pressure acting on the plate was derived by Albano and Rodden (1969). The series of spatial functions is used to approximate a pressure. The vortex method is used to analyze the aerodynamics of wings by Katz (1985). Morino et al. (1975) suggested the method to predict the flowing of finite thickness curved surfaces. Morino and Kuo (1974) derived the integro-differential equation to describe the plate interaction with the compressible gas flow. Djojodihardjo and Widnall (1969) suggested the numerical approach to solve the singular integral equation with respect to a circulation density. Hess (1975) proposed the new method to analyze a gas flowing of three-dimensional bodies. Landahl and Stark (1968) investigated different types of the singular integral equations with respect to both a circulation density and a pressure. The advantages and shortcomings of these integral equations were discussed. Strganac and Mook (1990) analyzed the wings flowing at arbitrary angle of attack. The vortex method was used to solve the aerodynamic problem. Mook and Dong (1994) suggested the methods for calculations of incompressible flows past airfoils and their wakes. The properties of the wake behind airfoils were considered. Eloy et al. (2007) assumed that the flutter mode is two-dimensional but the potential flow is assumed to be three-dimensional. Using the Galerkin method and the Fourier transformations, the flutter mode is predicted. Preidikman and Mook (1998) analyzed the dynamics of the rigid plate with two degrees of freedoms. The method of discrete vortices was applied to predict the wind loads acting on the plate. The self-sustained vibrations of a wing are absorbed using the saturation phenomenon (Hall et al. 2001). Three-dimensional vortex lattice method was applied to describe the aerodynamic problem. Watanabe et al. (2002) discussed different methods for the paper flutter analysis. Both the Navier-Stokes equations simulations and the potential flow analysis were considered to calculate unsteady lift forces. The authors concluded that the potential theory was enough to predict the paper flutter. Guo and Paidoussis (2000) analyzed the plate stability. The Fourier transformation was used to solve the Laplace equation with respect to the velocity potential. Ellen (1972) considered the clamped plate flowing by an incompressible gas. The pressure drop is described by the integral of the plate displacements. The plate divergence was analyzed analytically. Kornecki et al. (1976) and Huang (1995) considered flutter of cantilever plates using Theodorsen theory. Shayo (1980) analyzed the linear vibrations of the plate interacting with moving gas. The singular integral equations with respect to the pressure acting on the lifting surface were treated in the book (Dowell et al. 1995). The self-sustained vibrations of the plates with geometrical nonlinearity flowing by gas were studied in the papers (Attar and

Dowell 2003; Tang et al. 1999b; Tang and Dowell 2002; Tang et al. 1999a). The vortex lattice method was used to simulate a potential stream. The pressure drop on the vibrating plate was analyzed in the paper (Breslavsky 2011). The almost periodic and the chaotic vibrations of the plates with internal resonances flowing by gas were considered in the paper (Avramov 2012). The method of discrete vortices for inviscid potential flows analysis was treated in the books (Belotserkovskii and Lifanov 1993; Lifanov et al. 2004).

Thus, the singular integral equations with respect to a circulation density are generally used to describe the interactions of thin-walled structures with a stream. Due to the wake formation, transients are observed and analyzed mandatory. Numerical analysis of these motions leads to significant computational burden.

The system of the singular integral equations with respect to the aerodynamic derivatives of the plate pressure drop is derived in this paper. Then there is no necessity to account the wake shed from the trailing edge. In this case, the numerical analysis of the plate vibrations in gas flow is simpler than the analysis, which is used the singular integral equations with respect to a circulation density. The numerical method for the solution of the singular integral equations with respect to the aerodynamic derivatives of the pressure drop is suggested. Validity of the plates dynamic stability analysis is verified by comparison with the results of others researchers.

Many models of plate vibrations in stream exist. The plates of wing-type are described by 2D models (Tang et al. 1999a, b). The plates of flag-type are described by 1D models (Eloy et al. 2007; Tang and Dowell 2002). The general method for analysis of plate stability in stream is suggested in this paper.

12.2 Equations of Plate Motions

The flexural vibrations of the rectangular plates in stream (Fig. 12.1) are analyzed. Transversal vibrations of the plates are described by the function $w(x, y, t)$, which satisfies the following partial differential equation:

$$\frac{h^2}{12}\nabla^4 w + \frac{1-\nu^2}{E}\left(\rho\,\ddot{w} + c\dot{w} + \frac{\Delta\, p(x, y, t)}{h}\right) = 0, \tag{12.1}$$

where $\nabla^4 w = \frac{\partial^4 w}{\partial x^4} + 2\frac{\partial^4 w}{\partial x^2 \partial y^2} + \frac{\partial^4 w}{\partial y^4}$; $\ddot{w} = \frac{\partial^2 w}{\partial t^2}$; h is plate thickness; E, ν are Young's modulus and the Poisson's ratio; ρ is the material density; c is the coefficient of the material damping; $\Delta\, p(x, y, t)$ is a pressure drop on the plate.

The plate dynamics is expanded by using the eigenmodes $\psi_j(x, y)$:

$$w(x, y, t) = \sum_{j=1}^{N_1} q_j(t)\, \psi_j(x, y)\,, \tag{12.2}$$

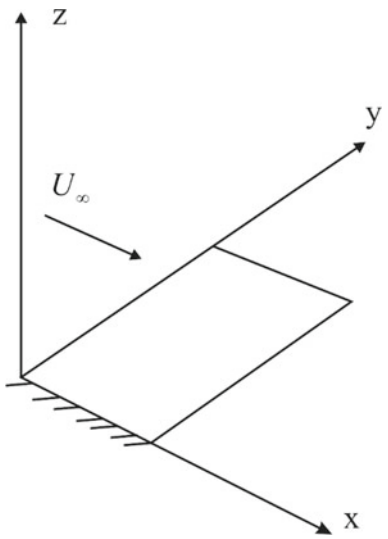

Fig. 12.1 Sketch of the system

where $q_j(t)$ are the generalized coordinates of the plate. It is assumed, that the plate vibrations are single harmonic:

$$q_j(t) \approx \gamma_j \cos(\omega t) + \delta_j \sin(\omega t); \quad j = 1, \ldots, N_1 . \tag{12.3}$$

12.3 System of Singular Integral Equations with Respect to Aerodynamic Derivatives of Pressure Drop

The plate is streamed by three-dimensional, potential, inviscid and incompressible gas. On significant distance from a plate, the flow has constant velocity U_∞, which is parallel to x axis. The projections of the flow velocities on x, y, z axes are denoted by $u(x, y, z, t)$; $v(x, y, z, t)$; $w(x, y, z, t)$, respectively. The velocity potential $\varphi(x, y, z, t)$ satisfies the following equations: $u = U_\infty + \frac{\partial \varphi}{\partial x}$; $v = \frac{\partial \varphi}{\partial y}$; $w = \frac{\partial \varphi}{\partial z}$. The velocity potential and pressure $p(x, y, z, t)$ satisfy the Laplace equations:

$$\nabla^2 \varphi = 0; \ \nabla^2 p = 0, \tag{12.4}$$

where $\nabla^2 \varphi = \frac{\partial^2 \varphi}{\partial x^2} + \frac{\partial^2 \varphi}{\partial y^2} + \frac{\partial^2 \varphi}{\partial z^2}$.

The boundary conditions for the Laplace equation (12.4) are considered. The Sommerfeld radiation condition is fulfilled:

$$\lim_{x^2+y^2+z^2 \to \infty} \text{grad}\, \varphi = 0. \tag{12.5}$$

The no penetration boundary condition satisfies on the plate surface:

$$\left.\frac{\partial \varphi}{\partial z}\right|_{z=0} = \frac{\partial w}{\partial t} + U_\infty \frac{\partial w}{\partial x}. \tag{12.6}$$

The pressure drop

$$\Delta p(x, y, t) = p(x, y, z)|_{z=0^+} - p(x, y, z)|_{z=0^-}$$

is equal to zero outside the plate on the plane $z = 0$. The pressure drop is equal to zero on the plate boundary ∂S:

$$\Delta p|_{\partial S} = 0. \tag{12.7}$$

The aerodynamic derivatives (Belotserkovskii and Lifanov 1993; Lifanov et al. 2004) are used to calculate the flow perturbations induced by the plate vibrations:

$$\varphi(x, y, z, t) = \sum_{j=1}^{N_1} \left[\varphi_j^{(0)}(x, y, z) q_j(t) + \varphi_j^{(1)}(x, y, z) \dot{q}_j(t) \right]; \tag{12.8}$$

$$p(x, y, z, t) = \sum_{j=1}^{N_1} \left[p_j^{(0)}(x, y, z) q_j(t) + p_j^{(1)}(x, y, z) \dot{q}_j(t) \right]. \tag{12.9}$$

Following (Belotserkovskii and Skripach 1975), the functions $\varphi_j^{(0)}(x, y, z)$, $\varphi_j^{(1)}(x, y, z)$, $p_j^{(0)}(x, y, z)$, $p_j^{(1)}(x, y, z)$ satisfy the Laplace equations:

$$\nabla^2 \varphi_j^{(k)} = 0; \tag{12.10}$$

$$\nabla^2 p_j^{(k)} = 0; \; k = 0, 1; \; j = 1, \ldots, N_1. \tag{12.11}$$

Index j indicates the number of eigenmode, which induce the pressure drop. The solutions of Eqs. (12.10, 12.11) satisfy the boundary conditions (12.5, 12.6, 12.7). The solutions of Eq. (12.11) take the following form (Dowell et al. 1995):

$$p_j^{(k)}(x, y, z) = \frac{1}{4\pi} \int_S \int \Delta p_j^{(k)}(x_1, y_1) \left[\frac{\partial}{\partial z_1} \left(\frac{1}{r} \right) \right]_{z_1=0} \mathrm{d}x_1 \mathrm{d}y_1, \tag{12.12}$$

where $r = \sqrt{(x - x_1)^2 + (y - y_1)^2 + (z - z_1)^2}$; S is region of the plate middle plane; $\Delta p_j^{(k)}(x_1, y_1) = p_j^{(k)}(x_1, y_1, z_1)|_{Z_1=0^+} - p_j^{(k)}(x_1, y_1, z_1)|_{Z_1=0^-}$ are aerodynamic derivatives of the plate pressure drop; x_1, y_1, z_1 are integration variables.

Bernoulli's equation is used in the following form:

$$p(x,y,z) = -\rho_\infty\left(\frac{\partial\varphi(x,y,z,t)}{\partial t} + U_\infty\frac{\partial\varphi(x,y,z,t)}{\partial x}\right), \tag{12.13}$$

where ρ_∞ is a gas density. Equations (12.8, 12.9) is substituted into Eq. (12.13). As a result, the following system of the partial differential equations is obtained:

$$\begin{aligned} U_\infty\frac{\partial\varphi_j^{(0)}}{\partial x} - \omega^2\varphi_j^{(1)} &= -\frac{p_j^{(0)}}{\rho_\infty};\\ U_\infty\frac{\partial\varphi_j^{(1)}}{\partial x} + \varphi_j^{(0)} &= -\frac{p_j^{(1)}}{\rho_\infty}. \end{aligned} \tag{12.14}$$

The method of constants variation is used to solve Eq. (12.13). The solution of this system takes the following form:

$$\begin{aligned} \varphi_j^{(0)}(x,y,z) &= B_j^{(1)}(x,y,z)\exp\left(i\frac{\omega}{U_\infty}x\right) + B_j^{(2)}(x,y,z)\exp\left(-i\frac{\omega}{U_\infty}x\right);\\ \varphi_j^{(1)}(x,y,z) &= \frac{i}{\omega}B_j^{(1)}(x,y,z)\exp\left(i\frac{\omega}{U_\infty}x\right) - \frac{i}{\omega}B_j^{(2)}(x,y,z)\exp\left(-i\frac{\omega}{U_\infty}x\right), \end{aligned} \tag{12.15}$$

where i is the imaginary unit. Equation (12.15) is substituted into (12.14). As a result, it is derived:

$$\begin{aligned} 2U_\infty\rho_\infty\frac{\partial B_j^{(1)}(x,y,z)}{\partial x} &= \left[i\omega\, p_j^{(1)}(x,y,z) - p_j^{(0)}(x,y,z)\right]\exp\left[-i\frac{\omega}{U_\infty}x\right];\\ 2U_\infty\rho_\infty\frac{\partial B_j^{(2)}(x,y,z)}{\partial x} &= -\left[i\omega\, p_j^{(1)}(x,y,z) + p_j^{(0)}(x,y,z)\right]\exp\left[i\frac{\omega}{U_\infty}x\right]. \end{aligned} \tag{12.16}$$

The integration of Eq. (12.16) is carried out using the Sommerfeld conditions (12.5). The results are substituted into (12.15). It is obtained:

$$\begin{aligned} \varphi_j^{(1)}(x,y,z) = -\frac{1}{U_\infty\rho_\infty\omega}\int\limits_{-\infty}^{x}\Bigg[&\omega p_j^{(1)}(\xi,y,z)\cos\left(\frac{\omega}{U_\infty}(\xi-x)\right)\\ &+ p_j^{(0)}(\xi,y,z)\sin\left(\frac{\omega}{U_\infty}(\xi-x)\right)\Bigg]\mathrm{d}\xi;\\ \varphi_j^{(0)}(x,y,z) = \frac{1}{U_\infty\rho_\infty}\int\limits_{-\infty}^{x}\Bigg[&-p_j^{(0)}(\xi,y,z)\cos\left(\frac{\omega}{U_\infty}(\xi-x)\right)\\ &+ \omega p_j^{(1)}(\xi,y,z)\sin\left(\frac{\omega}{U_\infty}(\xi-x)\right)\Bigg]\mathrm{d}\xi. \end{aligned} \tag{12.17}$$

The expansions (12.8, 12.9) are substituted into the boundary condition (12.6). As a result, the time-independent boundary conditions are obtained:

$$\left.\frac{\partial \varphi_j^{(0)}}{\partial z}\right|_{z=0} = U_\infty \frac{\partial \psi_j}{\partial x}\ ; \tag{12.18}$$

$$\left.\frac{\partial \varphi_j^{(1)}}{\partial z}\right|_{z=0} = \psi_j. \tag{12.19}$$

The solution (12.12) is substituted into Eq. (12.17) and the result is substituted into (12.8, 12.9). As a result, the following system of the singular integral equations is obtained:

$$\begin{aligned} 4\pi U_\infty^2 \rho_\infty \frac{\partial \psi_j(x,y)}{\partial x} &= -\omega \iint\limits_S \Delta p_j^{(1)}(x_1,y_1) K_S(x-x_1,y-y_1)\mathrm{d}x_1\mathrm{d}y_1 \\ &\quad + \iint\limits_S \Delta p_j^{(0)}(x_1,y_1) K_C(x-x_1,y-y_1)\mathrm{d}x_1\mathrm{d}y_1\ ; \\ 4\pi U_\infty \rho_\infty \omega \psi_j(x,y) &= \omega \iint\limits_S \Delta p_j^{(1)}(x_1,y_1) K_C(x-x_1,y-y_1)\mathrm{d}x_1\mathrm{d}y_1 \\ &\quad + \iint\limits_S \Delta p_j^{(0)}(x_1,y_1) K_S(x-x_1,y-y_1)\mathrm{d}x_1\mathrm{d}y_1, \end{aligned} \tag{12.20}$$

where

$$\begin{aligned} K_C(x-x_1,y-y_1) &= -\int\limits_{-\infty}^{x-x_1} \frac{\cos\frac{\omega(\lambda+x_1-x)}{U_\infty}}{\left[\lambda^2+(y-y_1)^2\right]^{3/2}}\mathrm{d}\lambda; \\ K_S(x-x_1,y-y_1) &= -\int\limits_{-\infty}^{x-x_1} \frac{\sin\frac{\omega(\lambda+x_1-x)}{U_\infty}}{\left[\lambda^2+(y-y_1)^2\right]^{3/2}}\mathrm{d}\lambda. \end{aligned} \tag{12.21}$$

The kernels $K_C(\tilde{x},\tilde{y})$ and $K_S(\tilde{x},\tilde{y})$ satisfy the following relations:

$$\lim_{\substack{\tilde{x}\to 0\\ \tilde{y}\to 0}} K_C(\tilde{x},\tilde{y}) = \infty;\ \lim_{\substack{\tilde{x}\to 0\\ \tilde{y}\to 0}} K_S(\tilde{x},\tilde{y}) = -\infty.$$

The following dimensionless variables and parameters are used:

$$\chi = \frac{\omega\, a}{U_\infty};\ \bar{\lambda} = \frac{\lambda}{a};\ \bar{x}_1 = \frac{x_1}{a};\ \bar{y}_1 = \frac{y_1}{b};\ \bar{x} = \frac{x}{a};\ \bar{y} = \frac{y}{b};$$

$$r = \frac{a}{b}\,;\ \tau = \omega\, t\,;\ \vartheta_i = \frac{q_i}{h}\,;$$
$$K_S = \frac{a\,\bar{K}_S}{b^3};\ K_C = \frac{a\bar{K}_C}{b^3}\,;\ \Delta\,\bar{p}_j^{(1)} = \frac{\omega\, a\Delta p_j^{(1)}}{\rho_\infty U_\infty^2}\,;\ \Delta\,\bar{p}_j^{(0)} = \frac{a\Delta p_j^{(0)}}{\rho_\infty U_\infty^2}, \tag{12.22}$$

where χ is the Strouhal number. The system of the singular integral Eq. (12.20) with respect to the dimensionless variables takes the following form:

$$\iint\limits_{\bar{S}} \left[-\Delta\,\bar{p}_j^{(1)}(\bar{x}_1, \bar{y}_1)\bar{K}_S(\bar{x}-\bar{x}_1, \bar{y}-\bar{y}_1) + \Delta\bar{p}_j^{(0)}(\bar{x}_1, \bar{y}_1)\bar{K}_C(\bar{x}-\bar{x}_1, \bar{y}-\bar{y}_1)\right]$$
$$\mathrm{d}\bar{x}_1\mathrm{d}\bar{y}_1 = \frac{\partial\psi_j(\bar{x}, \bar{y})}{\partial\bar{x}}\frac{4\pi}{r^2}; \tag{12.23}$$

$$\iint\limits_{\bar{S}} \left[-\Delta\,\bar{p}_j^{(1)}(\bar{x}_1, \bar{y}_1)\bar{K}_S(\bar{x}-\bar{x}_1, \bar{y}-\bar{y}_1) + \Delta\bar{p}_j^{(0)}(\bar{x}_1, \bar{y}_1)\bar{K}_C(\bar{x}-\bar{x}_1, \bar{y}-\bar{y}_1)\right]$$
$$\mathrm{d}\bar{x}_1\mathrm{d}\bar{y}_1 = \frac{\partial\psi_j(\bar{x}, \bar{y})}{\partial\bar{x}}\frac{4\pi}{r^2}\,; \tag{12.24}$$

$$\bar{K}_S(\bar{x}-\bar{x}_1, \bar{y}-\bar{y}_1) = -\int\limits_{-\infty}^{\bar{x}-\bar{x}_1} \frac{\sin\chi\left(\bar{\lambda}+\bar{x}_1-\bar{x}\right)}{\left[r^2\bar{\lambda}^2 + (\bar{y}-\bar{y}_1)^2\right]^{3/2}}\,\mathrm{d}\bar{\lambda}\,;$$
$$\bar{K}_C(\bar{x}-\bar{x}_1, \bar{y}-\bar{y}_1) = -\int\limits_{-\infty}^{\bar{x}-\bar{x}_1} \frac{\cos\ \chi\left(\bar{\lambda}+\bar{x}_1-\bar{x}\right)}{\left[r^2\bar{\lambda}^2 + (\bar{y}-\bar{y}_1)^2\right]^{3/2}}\,\mathrm{d}\bar{\lambda},$$

where $\bar{S}$ is the region of the plate middle plane with respect to dimensionless coordinates.

The kernels of the singular integral Eqs. (12.23, 12.24) satisfy the following relations:

$$\frac{\partial}{\partial\bar{x}}\bar{K}_s(\bar{x}-\bar{x}_1, \bar{y}-\bar{y}_1) = -\chi\ \bar{K}_c(\bar{x}-\bar{x}_1, \bar{y}-\bar{y}_1);$$
$$\frac{\partial}{\partial\bar{x}}\bar{K}_c(\bar{x}-\bar{x}_1, \bar{y}-\bar{y}_1) = -\left[r^2(\bar{x}-\bar{x}_1)^2 + (\bar{y}-\bar{y}_1)^2\right]^{-3/2} + \chi\ \bar{K}_s(\bar{x}-\bar{x}_1, \bar{y}-\bar{y}_1). \tag{12.25}$$

Equation (12.23) is differentiated with respect to $\bar{x}$ and the result is substituted into Eq. (12.24). As a result, the following singular integral equation is derived:

$$\iint\limits_{\bar{S}} \frac{\Delta\bar{p}_j^{(1)}(\bar{x}_1, \bar{y}_1)\mathrm{d}\bar{x}_1\mathrm{d}\bar{y}_1}{\left[r^2(\bar{x}-\bar{x}_1)^2 + (\bar{y}-\bar{y}_1)^2\right]^{3/2}} = -\frac{8\pi\chi}{r^2}\frac{\partial\psi_j(\bar{x}, \bar{y})}{\partial\bar{x}}\,. \tag{12.26}$$

The index j indicates on the number of eigenmode, which induced the pressure. Equation (12.24) is differentiated with respect to $\bar{x}$ and the result is substituted into (12.23). As a result, the following singular integral equation is derived:

$$\iint\limits_{\bar{S}} \frac{\Delta \bar{p}_j^{(0)}(\bar{x}_1, \bar{y}_1)\mathrm{d}\bar{x}_1\mathrm{d}\bar{y}_1}{\left[r^2(\bar{x}-\bar{x}_1)^2+(\bar{y}-\bar{y}_1)^2\right]^{3/2}} = \frac{4\pi}{r^2}\left[\chi^2\psi_j(\bar{x},\bar{y}) - \frac{\partial^2\psi_j(\bar{x},\bar{y})}{\partial\bar{x}^2}\right]. \quad (12.27)$$

Thus, the system of the singular integral equations with respect to the aerodynamic derivatives (12.26, 12.27) is derived. Equations (12.26) and (12.27) are solved independently. The vortex method (Belotserkovskii and Lifanov 1993; Lifanov et al. 2004) is used to solve these equations. If the solution of this system is obtained, the pressure drop on the plate is obtained using Eq. (12.9).

The system (12.26, 12.27) has several advantages in comparison with the frequently used singular integral equations with respect to the circulation density. The wake shed from the trailing edge is taken into account, if the system of singular integral equations with respect to the circulation density is solved. Then the plate transients are analyzed mandatory.

12.4 Finite Degrees of Freedom Model of Plates Vibrations

Equations (12.2) and (12.9) are substituted into (12.1). The Galerkin method is applied. As a result, the linear dynamical system with respect to the generalized coordinates $\vartheta_1, \vartheta_2, \ldots$ is derived. This dynamical system with respect to the dimensionless variables (12.22) takes the following form:

$$\sum_{j=1}^{N_1} R_{ij}\left(\chi^2\vartheta_j'' + \alpha\chi^2\vartheta_j' + \chi_1^2\Omega_j^2\vartheta_j\right) + \varepsilon\sum_{j=1}^{N_1}\left(A_{ij}\vartheta_j + B_{ij}\vartheta_j'\right) = 0;$$
$$i = 1, \ldots, N_1, \quad (12.28)$$

where

$$\vartheta_j' = \frac{\mathrm{d}\vartheta_j}{\mathrm{d}\tau};$$
$$R_{ij} = \iint\limits_{\bar{S}} \psi_j(\bar{x},\bar{y})\,\psi_i(\bar{x},\bar{y})\mathrm{d}\bar{x}\,\mathrm{d}\bar{y};$$
$$A_{ij} = \iint\limits_{\bar{S}} \bar{p}_j^{(0)}(\bar{x},\bar{y})\,\psi_i(\bar{x},\bar{y})\mathrm{d}\bar{x}\,\mathrm{d}\bar{y};$$

$$B_{ij} = \iint\limits_{\bar{S}} \bar{p}_j^{(1)}(\bar{x}, \bar{y})\, \psi_i(\bar{x}, \bar{y}) \mathrm{d}\bar{x}\, \mathrm{d}\bar{y};$$

$$\Omega_j = \frac{\omega_j}{\omega_1};\ \ \chi_1 = \frac{\omega_1 a}{U_\infty};\ \ \varepsilon = \frac{a\rho_\infty}{h\rho};\ \ \alpha = \frac{c}{\omega\rho}.$$

Stability analysis of the plate equilibrium is reduced to the investigations of the trivial equilibrium of the dynamical system (12.28). The characteristic exponents $\tilde{\lambda}$ are calculated to analyze this stability. The solution of the system (12.28) has the following form:

$$\left[\vartheta_j, \vartheta_j'\right] = \left[Q_j, V_j\right] \exp\left(\tilde{\lambda}\, t\right);\ \ j = 1, \ldots, N_1, \tag{12.29}$$

where Q_j, V_j are unknown parameters. The characteristic exponents are determined from the eigenvalue problem:

$$\begin{pmatrix} \mathbf{C^{(1)}} & \mathbf{C^{(2)}} \\ -\chi^2\mathbf{E} & 0 \end{pmatrix} \begin{pmatrix} \mathbf{V} \\ \mathbf{Q} \end{pmatrix} = -\lambda_1 \begin{pmatrix} \mathbf{V} \\ \mathbf{Q} \end{pmatrix}, \tag{12.30}$$

where ($\mathbf{E}$) is identity matrix;

$$\begin{aligned} \lambda_1 &= \chi^2\, \tilde{\lambda}; \\ \mathbf{C^{(1)}} &= \varepsilon \mathbf{R}^{-1}\mathbf{B} + \alpha\chi^2\mathbf{E}; \\ \mathbf{C^{(2)}} &= \varepsilon \mathbf{R}^{-1}\mathbf{A} + \chi_1^2\mathbf{\Omega^2}; \\ \mathbf{\Omega^2} &= \mathrm{diag}\left(\Omega_1^2; \ldots; \Omega_{N_1}^2\right); \\ \mathbf{Q} &= \left[Q_1, \ldots, Q_{N_1}\right];\ \mathbf{V} = \left[V_1, \ldots, V_{N_1}\right]; \\ \mathbf{A} &= \left\{A_{ij}\right\};\ \mathbf{B} = \left\{B_{ij}\right\};\ \mathbf{R} = \left\{R_{ij}\right\}. \end{aligned}$$

The values of the system parameters, where the Hopf bifurcation are observed, are called critical. Now the approach for the critical parameters calculation is considered. The parameter χ is preset with the step h_χ: $\chi^{(j)} = \chi_0 + jh_\chi$. For every value of $\chi^{(j)}$ the system of the singular integral Eqs. (12.26, 12.27) is solved. Using the results of the system (12.26, 12.27) solution, the finite degrees of freedom dynamical system (12.28) is obtained numerically. The critical values of the parameter χ_1 are calculated. If the system has critical parameters, two characteristic exponents are complex conjugate with zero real parts: $\tilde{\lambda}_{1,2} = \pm i\, \bar{\Omega}$. As a result of the calculations, the curve on the plane (χ, χ_1) is obtained. Only one point on this curve has the critical parameters (χ, χ_1).

The approach for determination of this point is considered. On the boundary of stability, the frequency of the system (12.28) vibrations is $\bar{\omega} = 1$. As follows from Eq. (12.30), the following relation satisfies at the Hopf bifurcation:

$$\bar{\Omega} = \chi^2.$$

This additional equation is used to obtain the critical parameters of the system (12.28).

12.5 Numerical Methods of Singular Integral Equation Solution

The singular integral Eqs. (12.26, 12.27) are solved independently. The numerical methods for their solution are identical.

The plate is split into n vertical and N horizontal bands. As a result, the plate consists of $n\,N$ rectangles (Fig. 12.2). The vertexes of these rectangles have the following coordinates: $x_k = k\,h_x\,;\ k = 1, \ldots, n\,;\ y_p = p\,h_y\,;\ p = 1, \ldots, N$. The region of the rectangle $k + n(p-1)$ is determined as:

$$S_{k+n(p-1)} = \left\{ (x, y) \in R^2 \middle| x_{k-1} < x < x_k;\ y_{p-1} < y < y_p \right\}. \tag{12.31}$$

The gravity center of the rectangle is denoted by $\left(\xi_k, \eta_p\right)$.

The rectangles are so small, that the functions $\Delta\,\bar{p}_j^{(1)}(\bar{x}_1,\ \bar{y}_1)$ and $\Delta\,\bar{p}_j^{(0)}(\bar{x}_1,\ \bar{y}_1)$ are assumed constants on them. These constants values are equal to the functions in the rectangles gravity centers:

$$\Delta\,\bar{p}_{0,j}^{[k+n(p-1)]} = \Delta\,\bar{p}_j^{(0)}\left(\xi_k, \eta_p\right)\,;$$
$$\Delta\,\bar{p}_{1,j}^{[k+n(p-1)]} = \Delta\,\bar{p}_j^{(1)}\left(\xi_k, \eta_p\right).$$

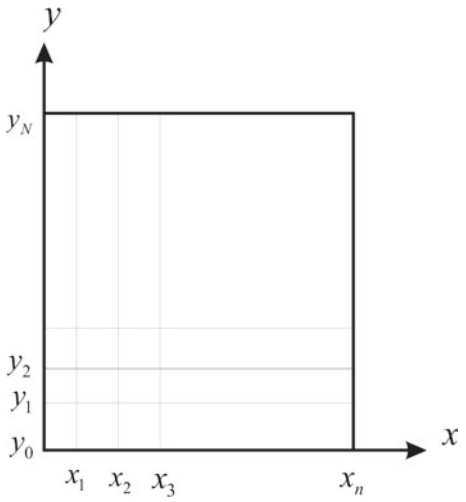

Fig. 12.2 The diagram of the plate discretization

The integral (12.26) is expressed as the sum of the integrals on all rectangles $S_{k+n(p-1)}$. Then Eq. (12.26) is satisfying in the collocation points $(\xi_l,\ \eta_m)$; $l = 1, \ldots, n$; $m = 1, \ldots, N$. As a result, the following system of linear algebraic equations with respect to $\Delta\, \bar{p}_{1,\,j}^{[\mu]}$; $\mu = 1, \ldots, nN$ is derived:

$$\sum_{k=1}^{n}\sum_{p=1}^{N} A_{l+n(m-1),k+n(p-1)}\, \Delta\, \bar{p}_{1,\,j}^{[k+n(p-1)]} = B_{l+n(m-1)}^{(1,\,j)}; \tag{12.32}$$

$$l = 1, \ldots, n;\ m = 1, \ldots, N,$$

where

$$A_{l+n(m-1),k+n(p-1)} = \frac{\sqrt{\left(\eta_m - y_p\right)^2 + r^2(\xi_l - x_{k-1})^2}}{\left(\eta_m - y_p\right)(\xi_l - x_{k-1})} - \frac{\sqrt{\left(\eta_m - y_p\right)^2 + r^2(\xi_l - x_k)^2}}{\left(\eta_m - y_p\right)(\xi_l - x_k)} + \frac{\sqrt{\left(\eta_m - y_{p-1}\right)^2 + r^2(\xi_l - x_k)^2}}{\left(\eta_m - y_{p-1}\right)(\xi_l - x_k)} - \frac{\sqrt{\left(\eta_m - y_{p-1}\right)^2 + r^2(\xi_l - x_{k-1})^2}}{\left(\eta_m - y_{p-1}\right)(\xi_l - x_{k-1})};$$

$$B_{l+n(m-1)}^{(1,\,j)} = -8\pi\chi\ \frac{\partial \psi_j(\bar{x}_l, \bar{y}_m)}{\partial \bar{x}}.$$

Thus, the solution of the singular integral Eq. (12.26) is reduced to the system of linear algebraic Eq. (12.32). The singular integral Eq. (12.27) is approximated by the following system of linear algebraic equations:

$$\sum_{k=1}^{n}\sum_{p=1}^{N} A_{l+n(m-1),k+n(p-1)}\, \Delta\, \bar{p}_{0,\,j}^{[k+n(p-1)]} = B_{l+n(m-1)}^{(0,\,j)};$$

$$B_{l+n(m-1)}^{(0,\,j)} = 4\pi\left[\chi^2 \psi_j(\bar{x}_l, \bar{y}_m) - \frac{\partial^2 \psi_j(\bar{x}_l, \bar{y}_m)}{\partial \bar{x}^2}\right].$$

12.6 Results of Numerical Analysis

Validation of the plate aeroelasticity by the system of the singular integral Eqs. (12.25, 12.26) and the numerical method for their solution is the main goal of stability numerical analysis. Dynamic stability of the plate (Fig. 12.3) is investigated numerically. This plate is analyzed in the paper (Tang et al. 2003). 1D model is used to analyze such plates in the papers (Eloy et al. 2007; Tang and Dowell 2002). However, 2D model is used to investigate this plate here. The following numerical values of the parameters are used:

$$E = 70.56 \cdot 10^9 \text{ Pa}; \ \rho = 2.84 \cdot 10^3 \text{ kg}/\text{m}^3;$$
$$\rho_\infty = 1.43 \text{ kg}/\text{m}^3; \ \nu = 0.3; \ h = 0.39 \cdot 10^{-3} \text{ m}; \ b = 0.127.$$

Figure 12.4 shows the first four modes of the plate vibrations at $r = 4$. Aerodynamic derivatives of the pressure, which are induced by these eigenmodes, are shown in Figs. 12.5 and 12.6.

Loss of the plate dynamic stability is analyzed. The critical stream velocity U_∞ and the vibrations frequency ω are calculated. The plate with $r = 2.12$ is considered. The critical stream velocity U_∞ and the plate vibrations frequency ω are calculated using the approach from Sect. 12.4. It is obtained: $U_\infty = 30.52 \text{ m/s}$; $\omega = 124 \text{ rad}/\text{s}$. The results of the calculations of the structure, which is treated in the paper (Tang et al. 2003), are $U_\infty = 29.5 \text{ m/s}$; $\omega = 141.3 \text{ rad}/\text{s}$. Thus, the results, which are published here, and the data from the paper (Tang et al. 2003) are close.

Changing the plate aspect ratio r, the loss of the plate dynamic stability is analyzed. Figure 12.7 shows the dependence of the critical stream velocity on the plate aspect ratio. The flutter onset frequency versus the plate aspect ratio is presented in Fig. 12.8. If the plate is lengthen, the stream velocity and the flutter onset frequency are

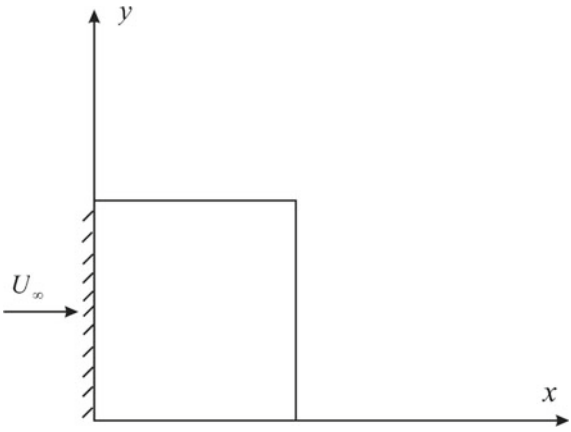

Fig. 12.3 Sketch of the plate

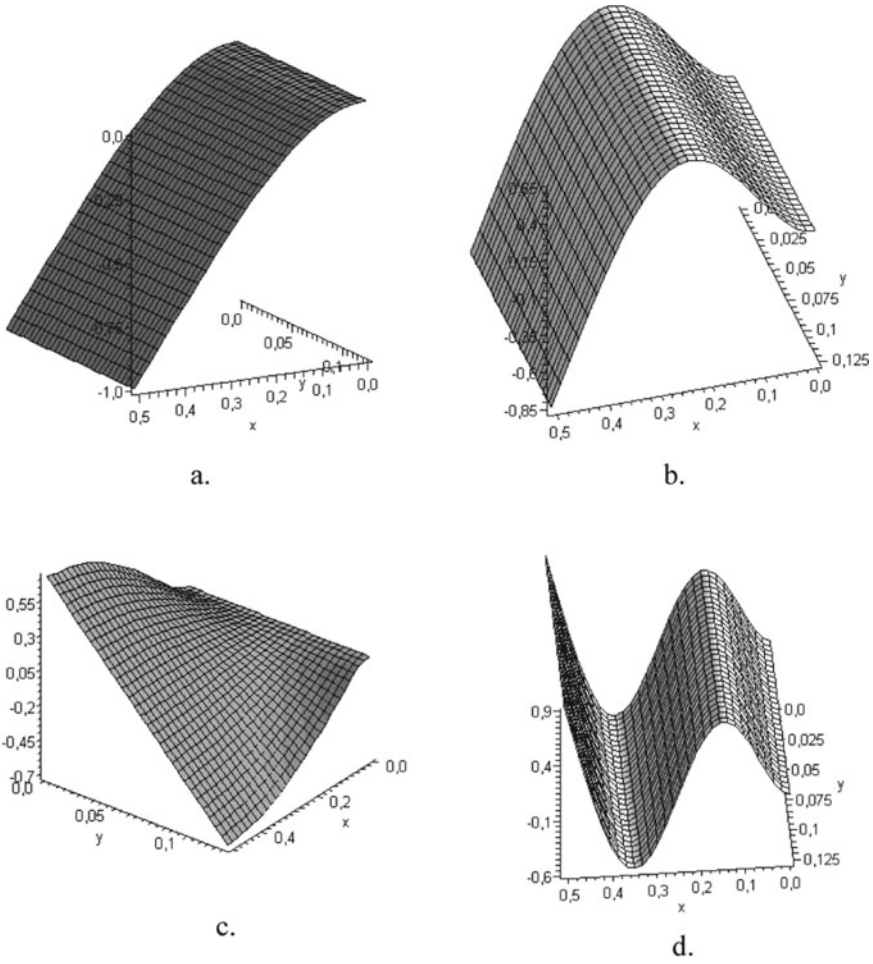

Fig. 12.4 The eigenmodes of the plate at $r = 4$. Figures **a**, **b**, **c**, **d** show the first, the second, the third and the fourth vibrations eigenmodes of the plate with the following parameters: $E = 70.56 \cdot 10^9$ Pa; $\rho = 2.84 \cdot 10^3\,\mathrm{kg}/\mathrm{m}^3$; $\rho_\infty = 1.43\ \mathrm{kg}/\mathrm{m}^3$; $\nu = 0.3$; $h = 0.39 \cdot 10^{-3}\,\mathrm{m}$; $b = 0.127$

decreased. The calculations results from the paper (Tang et al. 2003) are shown by point on Figs. 12.7 and 12.8.

The influence of damping coefficient α on parameters of flutter is analyzed. The results of analysis are shown in Figs. 12.9 and 12.10. Figure 12.9 shows the dependence of damping coefficient on critical stream velocity and Fig. 12.10 shows the dependence of flutter onset frequency on damping coefficient.

The data of stability analysis are obtained by 2D model and the results of 1D model analysis (Tang et al. 2003) are close.

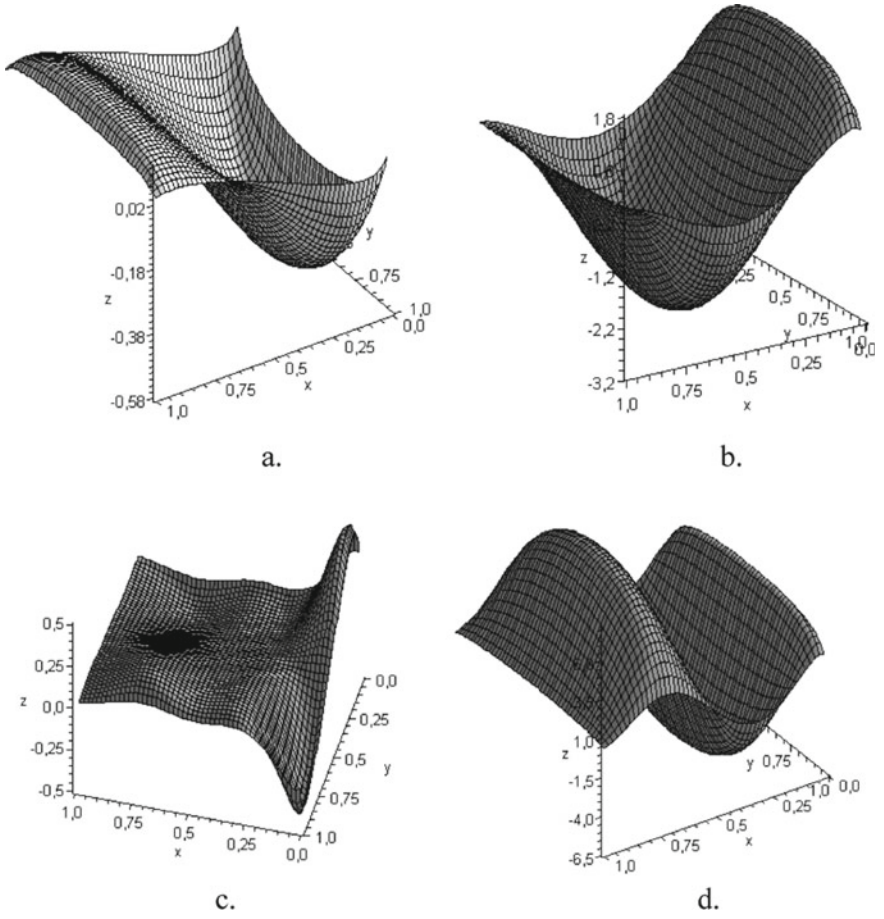

Fig. 12.5 The aerodynamic derivatives of the general coordinates. Figures **a**, **b**, **c**, **d** shows the aerodynamic derivatives induced by the first, the second, the third and the fourth eigenmodes of the plate with the following parameters: $E = 70.56 \cdot 10^9$ Pa; $\rho = 2.84 \cdot 10^3\,\mathrm{kg}/\mathrm{m}^3$; $\rho_\infty = 1.43\ \mathrm{kg}/\mathrm{m}^3$; $\nu = 0.3$; $h = 0.39 \cdot 10^{-3}$ m; $b = 0.127$

Dynamic stability of the plate (Fig. 12.1) is considered. The stream is parallel to x axis. The side $y = 0$ is clamped and all others sides are free. Aeroelastic stability of such plates is studied in the papers (Tang et al. 1999b; Avramov 2012). This system has the following numerical values of parameters:

$$a = b = 0.3\,\mathrm{m};\ h = 0.001\,\mathrm{m};\ E = 0.69 \cdot 10^{11}\ \mathrm{Pa};$$
$$\nu = 0.3;\ \rho = 2.7 \cdot 10^3\,\frac{\mathrm{kg}}{\mathrm{m}^3};\ \alpha = 0.005.$$

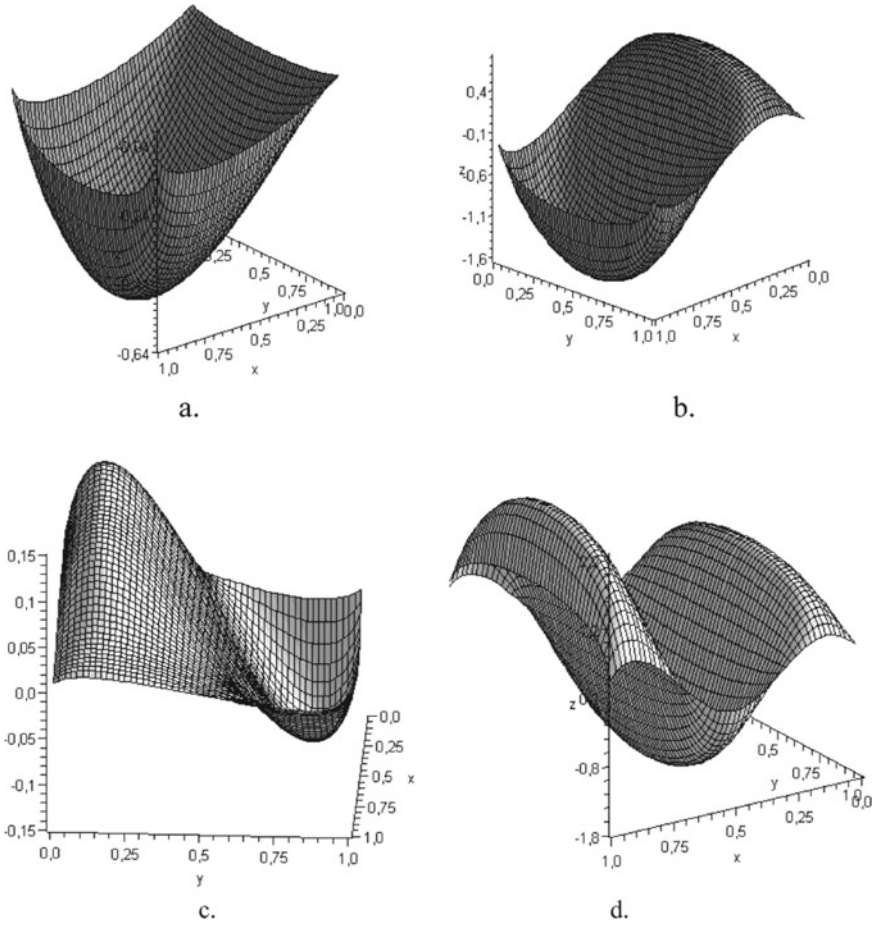

Fig. 12.6 The aerodynamic derivatives of the general velocities. Figures **a**, **b**, **c**, **d** show the aerodynamic derivatives induced by the first, the second, the third and the fourth eigenmodes with the following parameters: $E = 70.56 \cdot 10^9$ Pa; $\rho = 2.84 \cdot 10^3\,\mathrm{kg}/\mathrm{m}^3$; $\rho_\infty = 1.43\ \mathrm{kg}/\mathrm{m}^3$; $\nu = 0.3$; $h = 0.39 \cdot 10^{-3}$ m; $b = 0.127$

For the considered parameters the critical velocity is obtained: $V_\infty = 39.76$ m/s. The plate frequency for the critical system parameters is $\omega = 86.13$ rad/s. The following values of the plate critical velocity and frequency are published in Tang et al. (1999b): $V_\infty = 42.00$ m/s ; $\omega = 84.85$ rad/s. The results, which are published here, and the data from the paper (Tang et al. 1999b) are close.

Only dynamic instability of the plate is treated in this paper. The nonlinear vibrations of the structure (Avramov 2002, 2003, 2009; Avramov and Mikhlin 2004) are not considered.

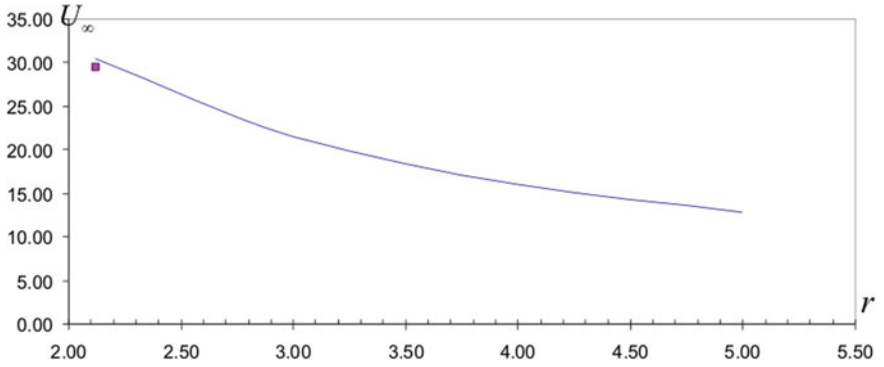

Fig. 12.7 The dependence of the critical stream velocity on the plate aspect ratio. The plate has the following parameters: $E = 70.56 \cdot 10^9$ Pa; $\rho = 2.84 \cdot 10^3\,\mathrm{kg}/\mathrm{m}^3$; $\rho_\infty = 1.43\ \mathrm{kg}/\mathrm{m}^3$; $\nu = 0.3$; $h = 0.39 \cdot 10^{-3}\,\mathrm{m}$; $b = 0.127$

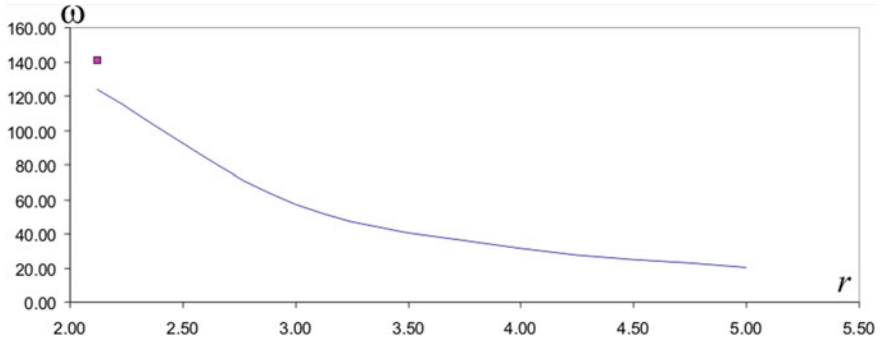

Fig. 12.8 The dependence of flutter onset frequency on the plate aspect ratio. The plate with the following parameters is considered: $E = 70.56 \cdot 10^9$ Pa; $\rho = 2.84 \cdot 10^3\,\mathrm{kg}/\mathrm{m}^3$; $\rho_\infty = 1.43\ \mathrm{kg}/\mathrm{m}^3$; $\nu = 0.3$; $h = 0.39 \cdot 10^{-3}\,\mathrm{m}$; $b = 0.127$

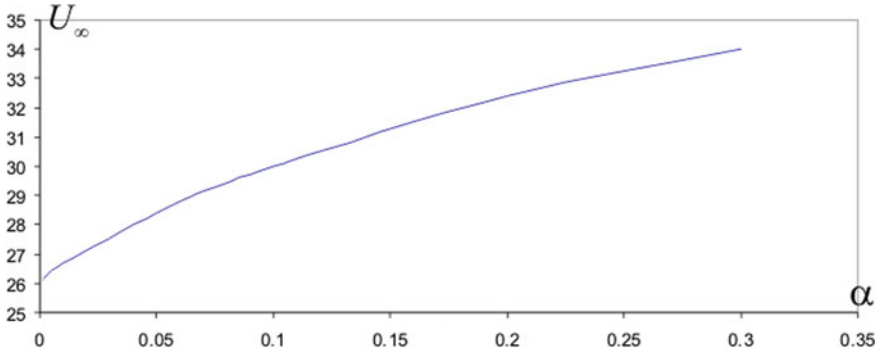

Fig. 12.9 The dependence of damping coefficients on critical stream velocity

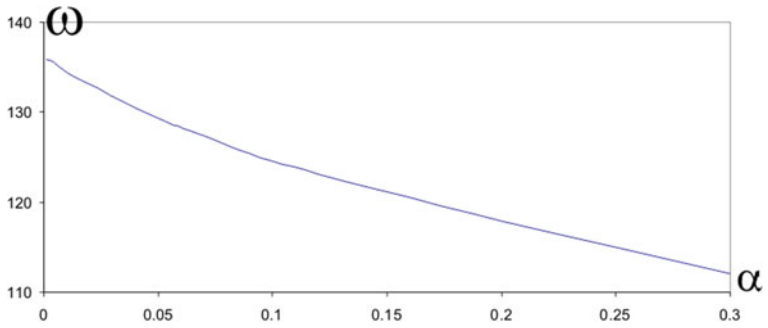

Fig. 12.10 The dependence of flutter onset frequency on the damping coefficient

12.7 Conclusions

The system of the singular integral equations with respect to the aerodynamic derivatives of pressure drop is suggested this paper. This system is very suitable for aeroelastic analysis, as there is unnecessary to analyze the wake shed from the trailing edge. Moreover, the approach for numerical solutions of the singular integral equations, based on the vortex method, is suggested.

For verification of the obtained system of singular integral equations and the method of their solution, the dynamic stability of several plates, which are treated in the previous papers, is analyzed. The obtained results are consistent with the data published by other researches.

The suggested system of singular integral equations will be used to analyze bifurcations and stability of nonlinear self-sustained vibrations of plates flowing by gas, using the modern methods of nonlinear dynamics.

Funding This study was particularly funded by National Research Foundation of Ukraine (grant number 128/02.2020).

References

Albano, E., Rodden, W.P.: A doublet-Lattice method for calculating lift distributions on oscillating surfaces in subsonic flows. AIAA J. **7**, 279–285 (1969)

Attar, P.J., Dowell, E.H.: A theoretical and experimental investigation of the effects of a steady angle of attack on the nonlinear flutter of a delta wing plate model. J. Fluids Struct. **17**, 243–259 (2003)

Avramov, K.V.: Nonlinear beam oscillations excited by lateral force at combination resonance. J. Sound Vib. **257**, 337–359 (2002)

Avramov, K.V.: Bifurcations of parametric oscillations of beams with three equilibrium. Acta Mech. **164**, 115–138 (2003)

Avramov, K.V.: Nonlinear modes of parametric vibrations and their applications to beams dynamics. J. Sound Vibr. **322**, 476–489 (2009)
Avramov, K.V., Mikhlin, Y.V.: Forced oscillations of a system containing a snap- through truss, close to its equilibrium position. Nonl. Dyn. **35**, 361–379 (2004)
Avramov, K.V., Strel'nikova, E.A., Pierre, C.: Resonant many-mode periodic and chaotic self-sustained aeroelastic vibrations of cantilever plates with geometrical nonlinearities in incompressible flow. Nonlinear Dyn. **70**, 1335–1354 (2012)
Belotserkovskii, S.M., Lifanov, I.K.: Method of discrete vortices. CRC Press, New York (1993)
Belotserkovskii, S.M., Skripach, B.K.: Aerodynamic derivatives of aircrafts and wings at subsonic flows. Nauka, Moscow (1975). (in Russian)
Breslavsky, I.D., Strel'nikova, E.A., Avramov, K.V.: Dynamics of shallow shells with geometrical nonlinearity interacting with fluid. Comput. Struct. **89**, 496–506 (2011)
Djojodihardjo, R.H., Widnall, S.E.: A numerical method for the calculation of nonlinear, unsteady lifting potential flow problems. AIAA J. **7**, 2001–2009 (1969)
Dowell, E.H., Curtiss, H.C., Scanlan, R.H., Sisto, F.: A modern course in aeroelasticity. Kluwer Academic Publishers, New York (1995)
Ellen, C.H.: Stability of clamed rectangular plates in uniform subsonic flow. AIAA J. **10**, 1716–1717 (1972)
Eloy, C., Souilliez, C., Schouveiler, L.: Flutter of a rectangular plate. J. Fluids Struct. **23**, 904–919 (2007)
Guo, C.Q., Paidoussis, M.P.: Stability of rectangular plates with free side-edges in two-dimensional inviscid channel flow. ASME J. Appl. Mech. **67**, 171–176 (2000)
Hall, B.D., Mook, D.T., Nayfeh, A.H., Preidikman, S.: Novel strategy for suppressing the flutter oscillations of aircraft wings. AIAA J. **39**, 1843–1850 (2001)
Hess, J.L.: Review of integral-equation techniques for solving potential-flow problems with emphasis of the surface-source method. Comput. Methods Appl. Mech. Eng. **5**, 145–196 (1975)
Huang, L.: Flutter of cantilevered plates in axial flow. J. Fluids Struct. **9**, 127–147 (1995)
Katz, J.: Calculation of the aerodynamic forces on automotive lifting surfaces. ASME J.Fluids Eng. **107**, 438–443 (1985)
Kornecki, A., Dowell, E.H., O'Brein, J.: On the aeroelastic instability of two-dimensional panels in uniform incompressible flow. J. Sound Vib. **47**, 163–178 (1976)
Landahl, M.T., Stark, V.J.E.: Numerical lifting-surface theory—problems and progress. AIAA J. **6**, 2049–2060 (1968)
Lifanov, I.K., Poltavskii, L.N., Vainikko, G.M.: Hypersingular integral equations and their applications. A CRC Press Company, New York (2004)
Mook, D.T., Dong, B.: Perspective: numerical simulations of wakes and blade-vortex interaction. ASME J. Fluids Eng. **116**, 5–21 (1994)
Morino, L., Kuo, C.C.: Subsonic potential aerodynamic for complex configurations: a general theory. AIAA J. **12**, 191–197 (1974)
Morino, L., Chen, L.T., Suciu, E.O.: Steady and oscillatory subsonic and supersonic aerodynamics around complex configuration. AIAA J. **13**, 368–374 (1975)
Preidikman, S., Mook, D.T.: On the development of a passive-damping system for wind-excited oscillations of long-span bridges. J. Wind Eng. Ind. Aerodyn. **77&78**, 443–456 (1998)
Shayo, L.K.: The stability of cantilever panels in uniform incompressible flow. J. Sound Vib. **68**, 341–350 (1980)
Strganac, T.W., Mook, D.T.: Numerical model of unsteady subsonic aeroelastic behavior. AIAA J. **28**, 903–909 (1990)
Tang, D., Dowell, E.H.: Limit cycle oscillations of two-dimensional panels in low subsonic flow. Int. J. Non-Linear Mech. **37**, 1199–1209 (2002)
Tang, D., Henry, J., Dowell, E.H.: Limit cycle oscillations of delta wing models in low subsonic flow. AIAA J. **37**, 1355–1362 (1999a)

Tang, D., Dowell, E.H., Hall, K.C.: Limit cycle oscillations of a cantilevered wing in low subsonic flow. AIAA J. **37**, 364–371 (1999b)
Tang, D.M., Yamamoto, H., Dowell, E.H.: Flutter and limit cycle oscillations of two-dimensional panels in three-dimensional axial flow. J. Fluids Struct. **17**, 225–242 (2003)
Watanabe, Y., Isogai, K., Suzuki, S., Sugihara, M.: A theoretical study of paper flutter. J. Fluids Struct. **16**, 543–560 (2002)